

Interim Technical Report for Second Year
on

Title of Project: “Development of Ceramic Laser Element”

AOARD Grant Number: 08- 4043

By Materials Team

Principal investigator: Akio Ikesue*

Researcher: Yan Lin Aung*

*World-Lab. Co. Ltd., 1-2-19-CSJ308 Mutsuno, Atsutaku, Nagoya 456-0023, Japan.

TEL&FAX:(052)-872-3950

poly-ikesue@s5.dion.ne.jp

Submission Date: Oct 15th, 2009

Submitted to

Dr. Kumar Jata, Program Manager

Asian Office of Aerospace Research & Development (AOARD)

7-23-17 Roppongi

Minato-ku, Tokyo 106-0032

TEL:(03)-5410-4409 FAX:(03)-5410-4407

kumar.jata@aoard.af.mil

Report Documentation Page			Form Approved OMB No. 0704-0188		
<p>Public reporting burden for the collection of information is estimated to average 1 hour per response, including the time for reviewing instructions, searching existing data sources, gathering and maintaining the data needed, and completing and reviewing the collection of information. Send comments regarding this burden estimate or any other aspect of this collection of information, including suggestions for reducing this burden, to Washington Headquarters Services, Directorate for Information Operations and Reports, 1215 Jefferson Davis Highway, Suite 1204, Arlington VA 22202-4302. Respondents should be aware that notwithstanding any other provision of law, no person shall be subject to a penalty for failing to comply with a collection of information if it does not display a currently valid OMB control number.</p>					
1. REPORT DATE 22 NOV 2009	2. REPORT TYPE FInal	3. DATES COVERED 18-09-2008 to 18-09-2009			
4. TITLE AND SUBTITLE Ceramics for high-power lasers			5a. CONTRACT NUMBER FA23860814043		
		5b. GRANT NUMBER			
		5c. PROGRAM ELEMENT NUMBER			
6. AUTHOR(S) Akio Ikesue			5d. PROJECT NUMBER		
		5e. TASK NUMBER			
		5f. WORK UNIT NUMBER			
7. PERFORMING ORGANIZATION NAME(S) AND ADDRESS(ES) World Lab Co., Ltd.,1-2-19-CSJ308 , Mutsuno, Atsuta-ku,Nagoya 456-0023,Japan,JP,456-0023			8. PERFORMING ORGANIZATION REPORT NUMBER N/A		
9. SPONSORING/MONITORING AGENCY NAME(S) AND ADDRESS(ES) AOARD, UNIT 45002, APO, AP, 96337-5002			10. SPONSOR/MONITOR'S ACRONYM(S) AOARD		
		11. SPONSOR/MONITOR'S REPORT NUMBER(S) AOARD-084043			
12. DISTRIBUTION/AVAILABILITY STATEMENT Approved for public release; distribution unlimited					
13. SUPPLEMENTARY NOTES					
14. ABSTRACT Practical laser generation from polycrystalline ceramic materials has become available; furthermore, it is expected that ceramic laser technology will completely surpass the conventional glass and single crystal laser technologies in the future. The newly fabricated ceramics have almost an ideal and perfect microstructure. Optical characterizations by laser showed that the scatter loss is almost zero for ceramic gain media. In the result, high optical quality ceramics showed high resistance to laser damage. Laser performance with very close to theoretical quantum efficiency was achieved from the developed high quality ceramic gain media, comparable to that of the Konoshima ceramics and commercial single crystal.					
15. SUBJECT TERMS ceramic laser, ceramic laser processing, Laser Materials Processing					
16. SECURITY CLASSIFICATION OF: a. REPORT unclassified			17. LIMITATION OF ABSTRACT Same as Report (SAR)	18. NUMBER OF PAGES 24	19a. NAME OF RESPONSIBLE PERSON
b. ABSTRACT unclassified	c. THIS PAGE unclassified				

Table of Contents

Abstract

1. Introduction	... p.3
2. Objective of the project	... p.4
3. Project schedule and targets	... p.4
4. Fabrication of high quality optical ceramics	... P.5
5. Observation in macro level (OM)	... P.7
6. Observation in micro level (SEM, EPMA)	... P.9
7. Observation in nano-level (HR-TEM)	... P.11
8. Characterization of powder mixture prepared by optimized process	... P.12
9. Optical characterization of laser ceramics	... P.15
10. Laser oscillation experiment	... P.19
11. Fabrication of waveguide laser elements	... P.21
12. Conclusions	... P.23
13. Future plan	... P.23
Acknowledgements	

Title of Project: “Development of Ceramic Laser Element”

Abstract

Practical laser generation from polycrystalline ceramic materials has become available; furthermore, it is expected that ceramic laser technology will completely surpass the conventional glass and single crystal laser technologies in the future. The newly fabricated ceramics have almost an ideal and perfect microstructure. Optical characterizations by laser showed that the scatter loss is almost zero for ceramic gain media. In the result, high optical quality ceramics showed high resistance to laser damage. Laser performance with very close to theoretical quantum efficiency was achieved from the developed high quality ceramic gain media, comparable to that of the konoshima ceramics and commercial single crystal.

Keywords: Transparent ceramics, transparent polycrystalline material, ceramic laser, high energy laser, high power laser, engineered ceramic composite, waveguide

1. Introduction

Solid-state laser is widely used in metal processing, medical applications, such as eye surgery, red-green-blue (RGB) light sources in laser printer and projectors, environmental instrumentation measurements, optical transmission systems and future nuclear fusion process. Single crystal or glass as a laser gain medium is generally used in the solid-state laser, which was originated from ruby laser by Maiman in 1960. Since the success of Geusic *et al.* in generating continuous-wave (c.w.) laser oscillation using Nd:YAG single crystal at room temperature in 1964, solid-state laser using single crystal has been continuously developed up till now.

The first laser oscillation using transparent Nd:YAG ceramics was demonstrated by Ikesue *et al.* in the 1990s with laser performance comparable to single-crystal laser oscillation. Recently, ceramic laser technology has emerged as a promising candidate because of its numerous advantages over single-crystal lasers. First, ceramic can be produced in large size which is attractive for high-power laser generation. Second, it can be processed into fibre-laser gain medium for generating laser with high beam quality, and also be processed into composite laser gain medium with complicated structures which are principally difficult to fabricate by conventional single crystal technology. The development of ceramic laser technology has led to the achievements of compact and highly efficient laser oscillation, ease of control of laser mode, generation of coherence beam with high focusing property. Moreover, the realization of high-power laser based on ceramic technology has brought the visions of ultrahigh-speed machining technology and nuclear fusion one step closer.

2. Objective of the project

The objective of the project is to develop a ceramic gain media for laser generation of high output power and high beam quality. Materials team is to fabricate ceramic laser materials having high optical quality and special configurations which are difficult to achieve from the conventional single crystal by melt-growth method and glass materials. In addition, base points for the development of next generation solid-state laser will be constituted. Basic technology of ceramic waveguide element, which is controlled with micro-structural refinement and macro- structural design, will be developed, and with the aid of analysis team, laser performances for high power output lasers will be evaluated with related to the thermo mechanical properties of the interface of waveguide designed ceramic laser element.

3. Project schedule and targets

The project will proceed on the basis of the materials development technology by materials team. Materials development will be involved; (1) materials synthesis and designing for the recognition of new functionality and high power laser generation, (2) machining of those prepared materials and surface treatment, (3) evaluation of basic properties of those prepared materials. It is planned to run as a three-year research project as shown in Fig.1, and targets for each year term are summarized in table 1. In the first year, media with lowest scatter loss will be prepared, and special laser elements will be prepared in the second and third year to achieve high output power ($\sim 1\text{kW}$) by focusing on waveguide designed media.

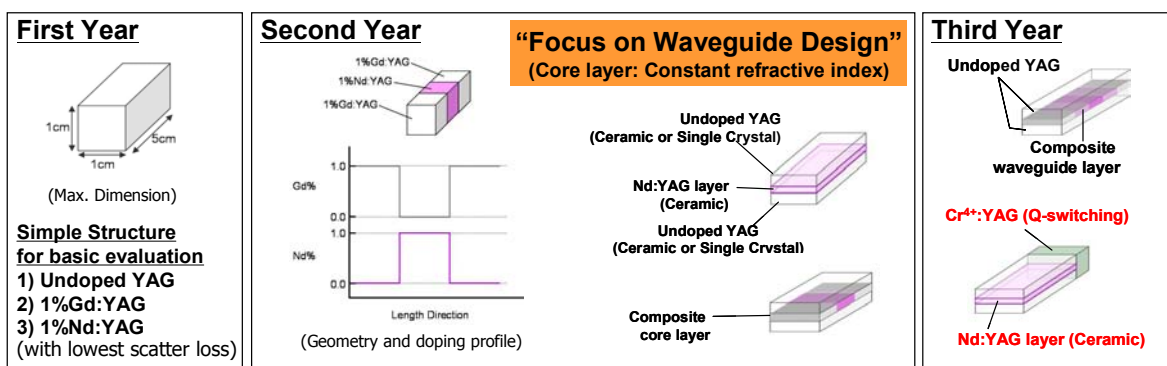


Fig 1. Laser gain media to be prepared in each year term of the project.

Table 1 Targets for each year term of the project

	Target Laser Output Power
First Year (2008)	Media with lowest scatter loss ($\sim 10^{-3}/\text{cm}$)
Second Year (2009)	$\sim 100\text{W}$
Third Year (2010)	300W $\sim 1\text{kW}$

4. Fabrication of high quality transparent ceramics

In the first year term, simple structure of undoped YAG, 1%Gd:YAG, and 1%Nd:YAG samples will be fabricated for basic evaluation. Laser gain media with lowest scattering loss will be prepared by modifying the ceramic process mainly on the microstructural refinement. The target of the optical quality of the materials is up to $10^{-3}/\text{cm}$ (0.001/cm) of scatter loss, which equal to the quality of commercialized Konoshima ceramic sample. Maximum dimension of each sample to be prepared for evaluation of basic properties is up to 1cmx1cmx5cm.

Solid-state reactive sintering process was applied to fabricate transparent ceramic laser gain media. Figure 2 shows the process, and figure 3 shows the SEM images of starting raw materials (high purity, 99.99%) used in this work. The primary particle sizes of Y₂O₃, Al₂O₃, and Nd₂O₃ were approximately 60nm, 300nm, and 400nm, respectively. These powders, blended with the stoichiometric ratio of garnet, were mixed and ball milled for one night in ethanol solvent with 0.5 mass% TEOS (tetraethyl orthosilicate) and a suitable amount of organic binder. The alcohol solvent was removed by spray drying the milled slurry, and at the same time granulated powders of about 50μm with spherical shapes were achieved.

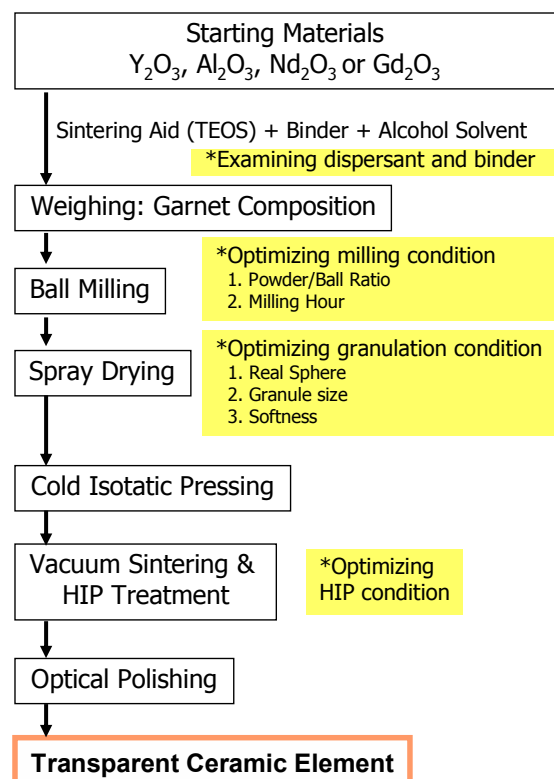


Fig.2 Fabrication process for the ceramic laser gain media.

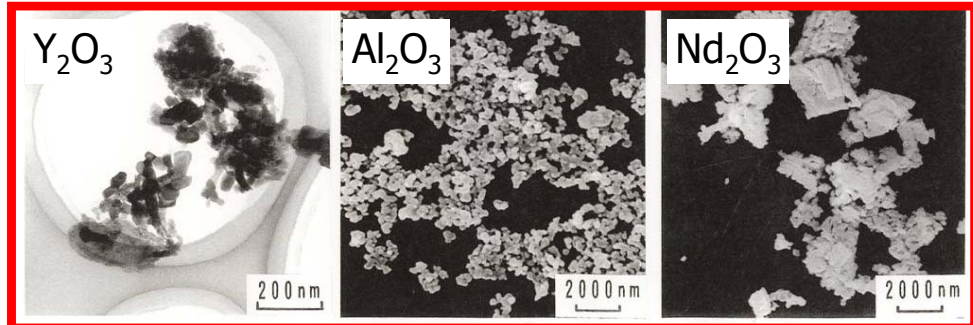


Fig.3 SEM images of the raw powder materials used as starting raw materials.

The spray-dried granulated powders were pressed with light pressure into a slab shape in a metal mold. The near-net-shaped sample was then cold isostatically pressed at 98–196 MPa, and a powder compact with a packing density of 50~55% of theoretical density was obtained. After heating of the pressed part to remove the organic component, the powder compact was sintered in vacuum (1×10^{-3} Pa) at 1750°C for a few-twenty hours to obtain transparent Nd:YAG ceramics. In addition, HIP (hot isostatic pressing) treatment was performed to further eliminate residual pores. After polishing, transparent ceramic laser gain media were achieved.

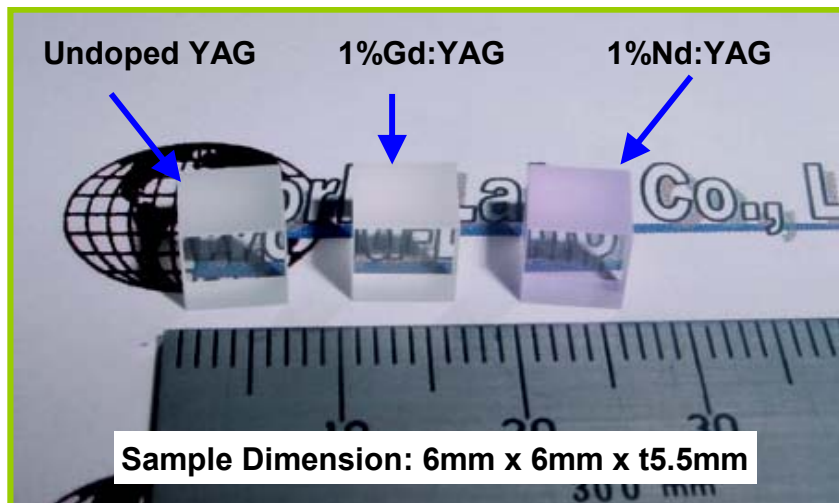


Fig.4 Appearance of fabricated samples for the evaluation of basic properties.

The transparent ceramic slabs (undoped YAG, 1%Gd:YAG, and 1%Nd:YAG) were machined into small blocks (dimension: 6mm x 6mm x t5.5mm) for optical measurements in macro level. The appearance of the fabricated samples is shown in Fig.4.

5. Observation in macro level

Polarized images of the whole samples are summarized in figure 5. Mechanical stress free condition was confirmed in all samples. Figure 6 shows the transmitted wavefront image of the all fabricated samples by interferometry. Almost straight fringes were observed, and this showed that the refractive index distribution in the whole sample is homogeneous.

Materials	Open Nicol	Cross Nicol
Undoped YAG		
1%Gd:YAG		
1%Nd:YAG		

Fig.5 Polarized images of the fabricated transparent ceramic samples.

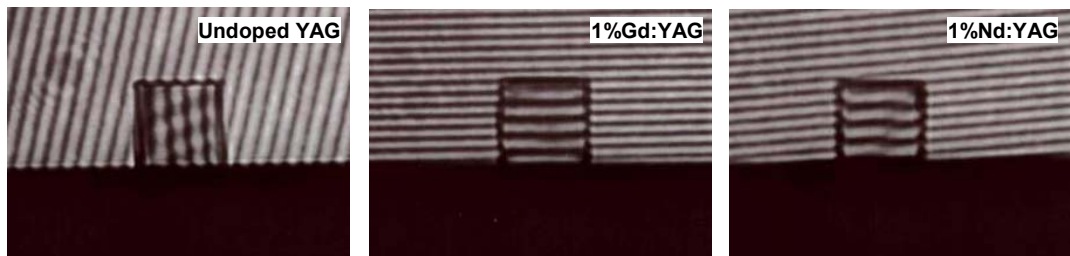


Fig.6 Transmitted wavefront image of the fabricated transparent ceramic samples.

In addition, in-line transmittance of each sample was measured from UV to visible and IR wavelength regions. Transmittance curves of each sample are shown in Fig.7. The in-line transmittance was as high as 84% transmittance, the theoretical value, which is equivalent to commercial 1.0 at.% Nd:YAG single crystal grown by the Czochralski method.

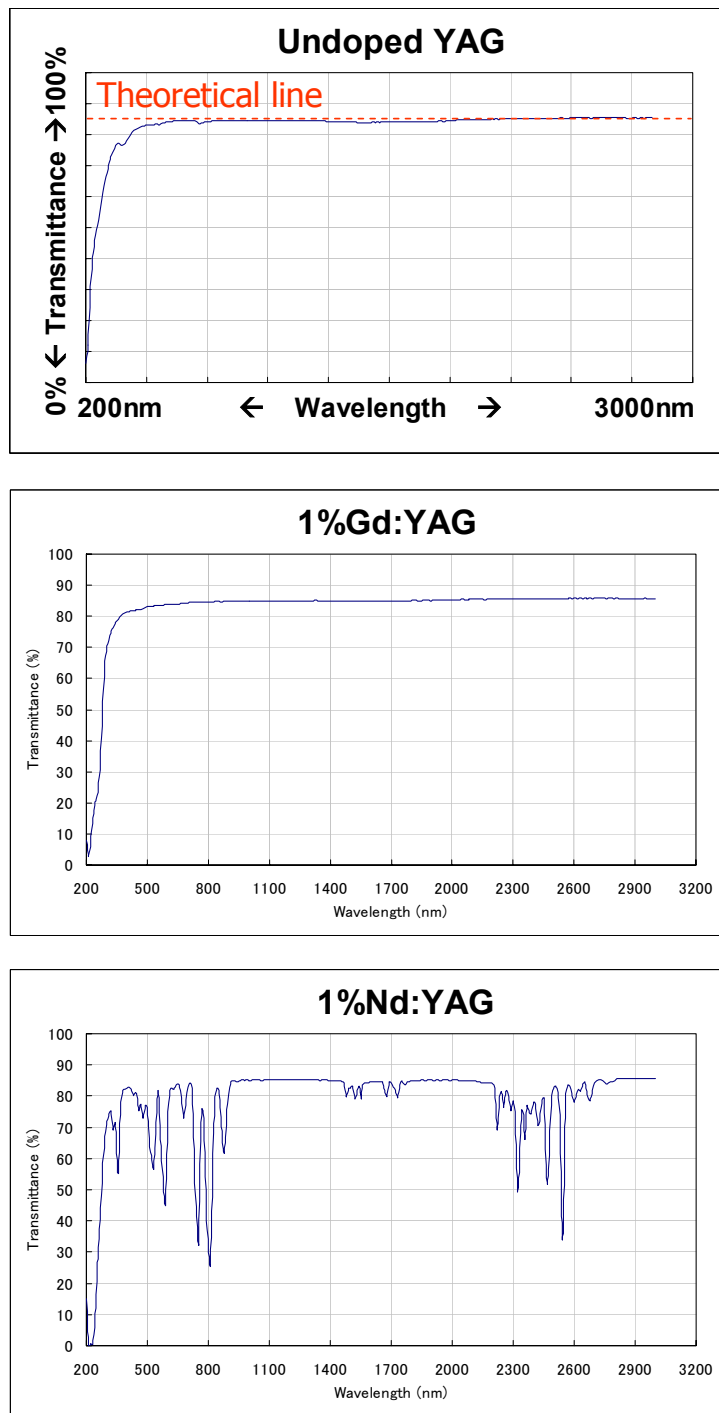


Fig.7 Transmittance curves of the fabricated transparent ceramic samples.

6. Observation in micro level

6.1 Under optical microscope (OM)

To check the grain size and microstructure of each transparent ceramics, one face polished samples were thermally etched at 1500C for 30 minutes, and they were observed under an optical microscope. Figure 8 shows the reflection microscopic images of thermal etched surface of each sample. Uniform microstructures and fine grain sizes of $\sim 10\mu\text{m}$ level were confirmed.

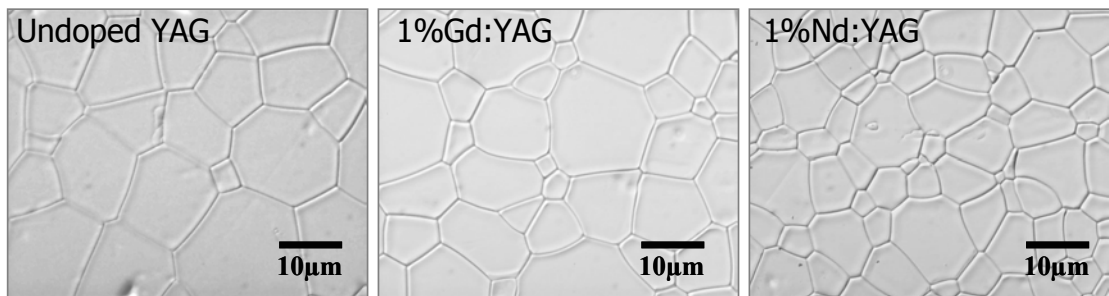


Fig.8 Thermal etched surfaces of the fabricated transparent ceramic samples observed under an optical microscope.

Figure 9 shows the transmitted polarized microscopy with open and cross nicol of each sample. No residual pores were observed, and very high optical homogeneity (birefringence free) was confirmed even at micron level.

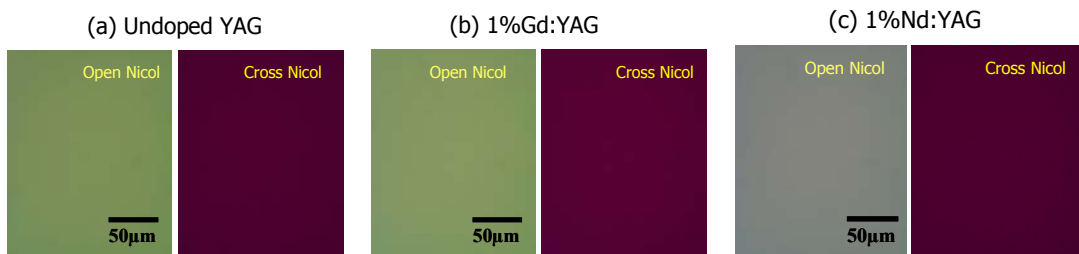


Fig.9 Transmitted polarized microscopy of the transparent ceramic samples.

6.2 By SEM and EPMA (electron probe micro analysis)

In order to check the internal grain size and microstructure, each of the sample were crushed down. Fracture surfaces of each sample were observed under SEM (see Fig.10). As observed under optical microscope, the internal microstructure was consistent with the surface microstructure. Moreover, almost no residual pores and no grain boundary phases were confirmed under SEM observation.

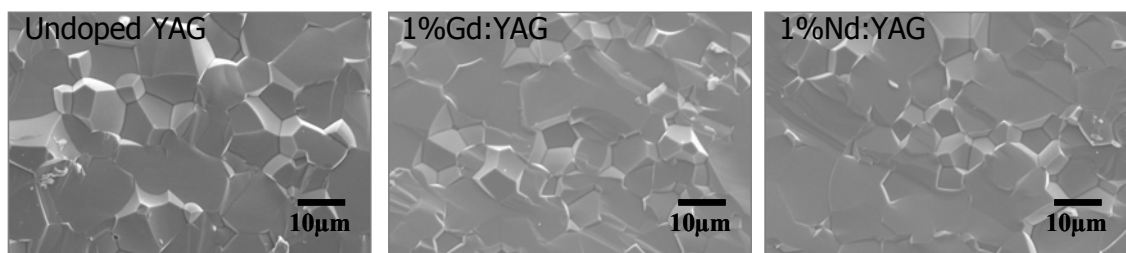


Fig.10 Fracture surfaces of the fabricated transparent ceramic samples by SEM observation.

Electron probe micro analysis was done for each sample in order to investigate the elemental (Y, Al, Gd, and Nd) distribution in micro level. The measured results were summarized in figure 11. It was confirmed that the dopant ions are homogeneously distributed and segregation of the dopant ions at macro-to-micro level was not observed.

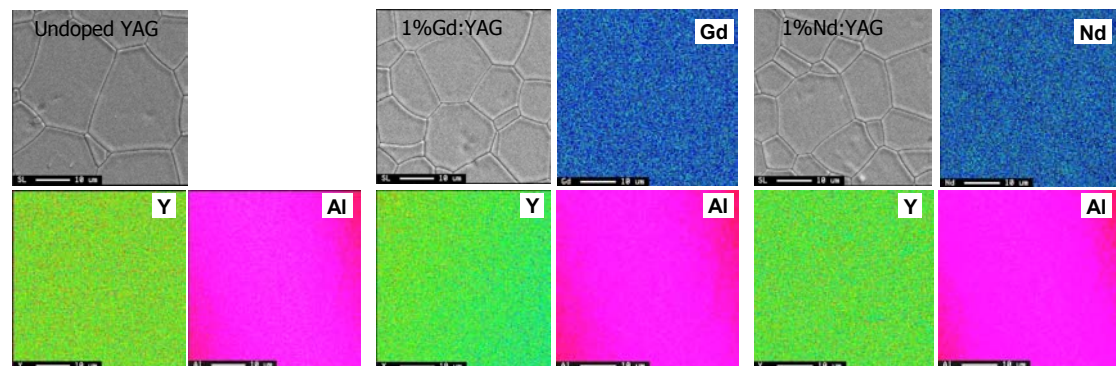


Fig.11 Electron probe micro analysis (EPMA) images of the fabricated transparent ceramic samples.

7. Observation in nano-level (High Resolution TEM analysis)

High resolution transmission electron microscopy was applied to investigate the lattice defects and formation of grain boundary phase was detected by using EDS (energy-dispersive spectroscopy) analysis. The results are summarized in figure 12. No atomic defects were recognized in the observed region of all samples. Clean grain boundaries (no secondary phases) were observed for all samples, except a few nano-meter thick amorphous layer (including SiO₂ from the sintering aid TEOS) was detected in some regions of grain boundaries. However, the thickness (2~3nm) of the amorphous layer is sufficiently small compared to the wavelength of the target laser wavelength (1064nm from Nd:YAG). Therefore, it can be considered that it may hardly effect on the optical quality of transparent ceramics.

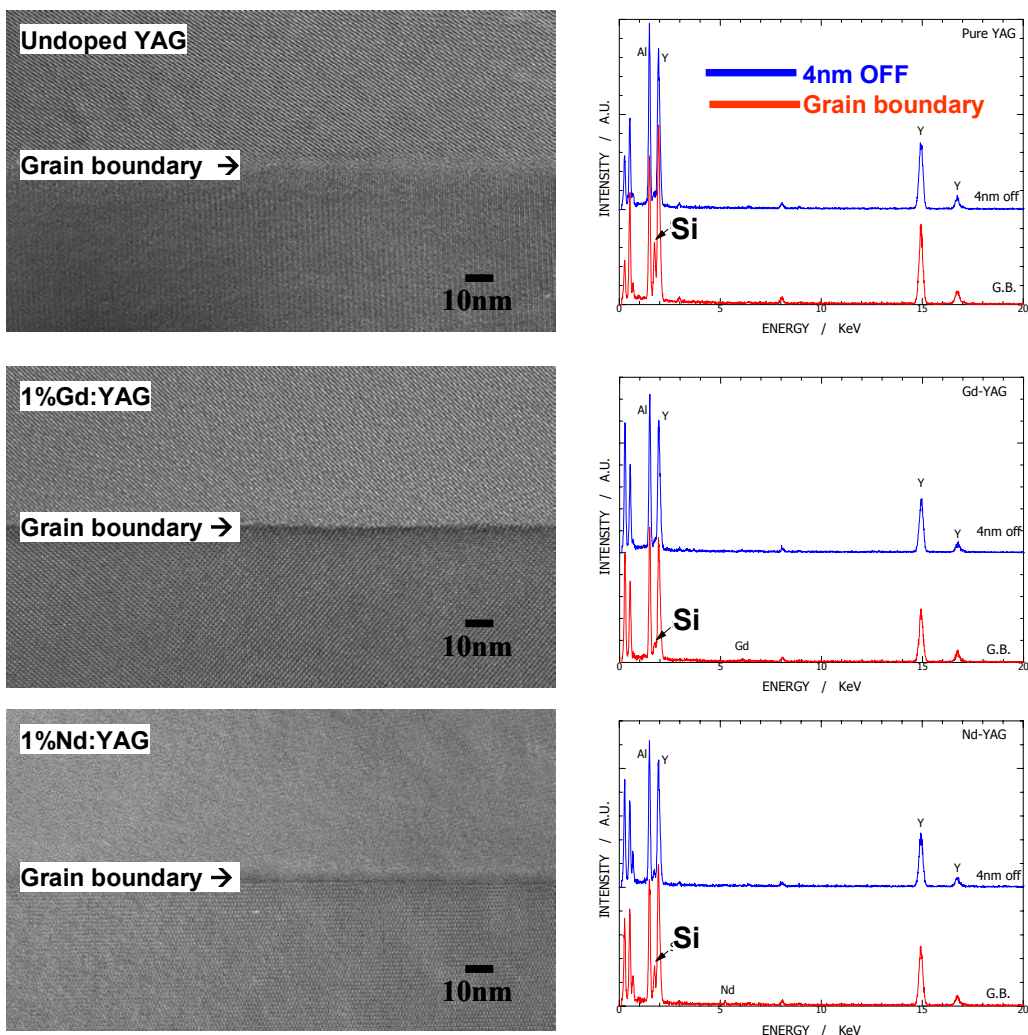


Fig.12 (Left) High resolution transmission electron microscopy (HR-TEM) images and (right) energy-dispersive spectroscopy (EDS) analysis results of the fabricated ceramic samples.

8. Characterization of powder mixture prepared by optimized process

Key technologies in the fabrication of high optical transparent ceramic by reactive sintering method are optimizing milling condition, granulation condition, cold-isostatic pressing condition, and hot-isostatic pressing condition etc. The physical properties of new powder mixture processed by optimized conditions were compared with that of the powder mixture prepared by conventional process. In addition, the crushing behavior of the spray-dried powder (granulated spherical powder) in powder compacts was investigated in order to form internal defect-free structure.

8.1 Particle distribution by laser diffractometry

Figure 13 shows the particle distribution curves of the ball-milled slurry prepared by current optimized process comparing with the conventional process. It was found that the finer particle distribution was achieved by optimizing the ball-milling condition. The homogeneity of the powder mixture was considered to be improved compared to the conventional powder mixture.

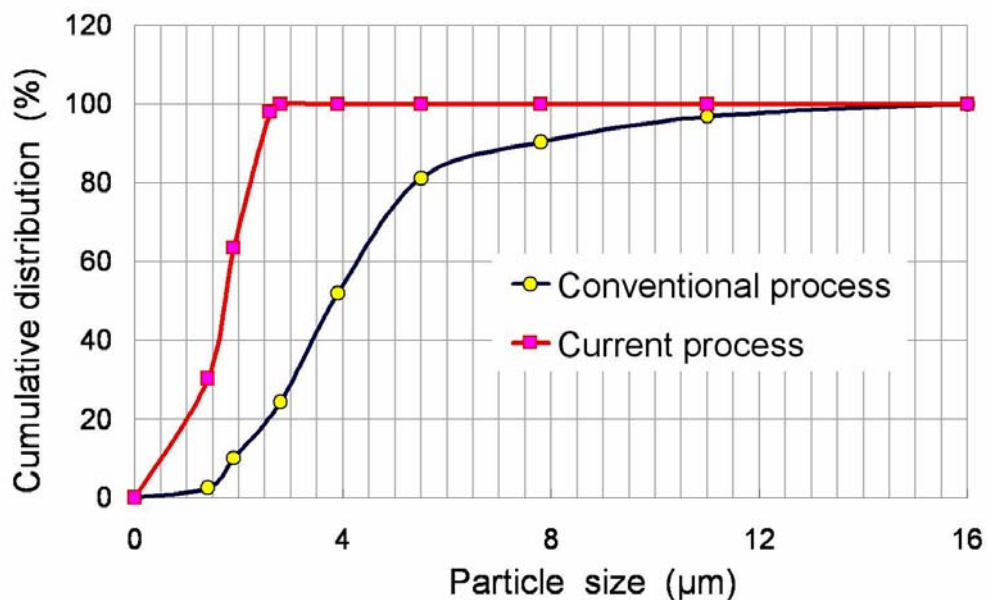


Fig.13 Particle distribution of ball-milled slurry obtained by current optimized process comparing to the conventional process.

8.2 Optimizing cold-isostatic pressing condition

By using a good combination of dispersant and binder, soft granules having spherical shapes were achieved by spray-drying the ball-milled slurry. The crushing behavior of the granulated powders in powder compact (tablet specimen) is summarized in Fig.14. It was confirmed that the spherical soft granules were easily crushed by lower pressure but some of the granules were not collapsed partially. When the CIP pressure was raised to 20MPa, the granules were completely collapsed. Accordingly, it was confirmed that the formation of soft and homogeneously mixed granules to produce defect-free internal structure.

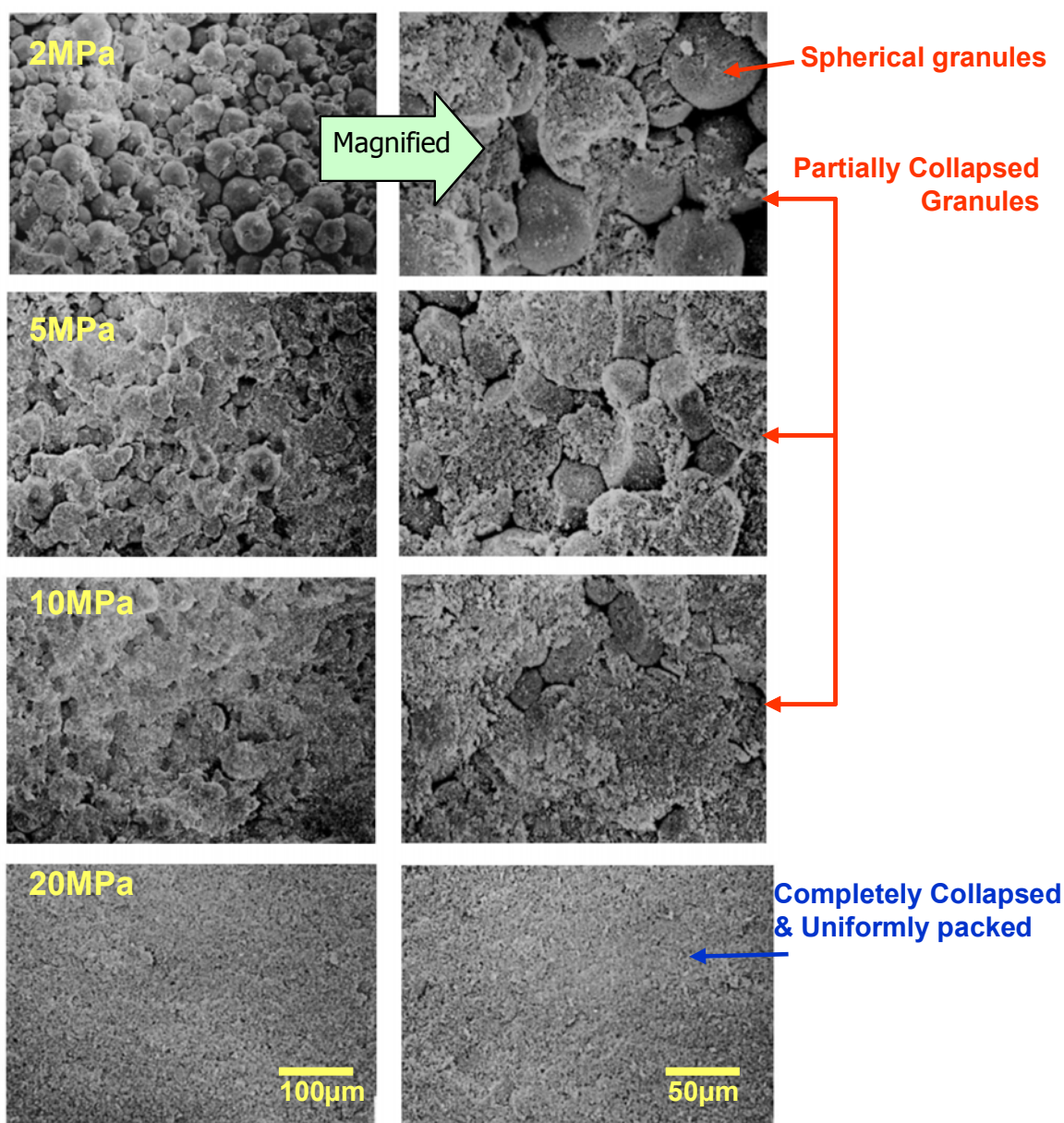


Fig.14 Fracture surfaces of specimen prepared by different cold-isostatic press condition.

8.3 Pore distribution by Mercury porosimetry

Mercury porosimetry was applied to measure the pore distribution in the powder compacts prepared with optimized CIP condition in comparison with the conventional process. Coarse defects such as pores and voids seen in the powder compact prepared by the conventional process were completely eliminated by processing soft granules and by optimizing the CIP condition. Defects generated in front-end process severely affected on the optical quality of the transparent ceramics. By changing the fundamental property of granules, uniform powder compact without internal voids (residual pores) were achieved, and finally defect-free transparent ceramics can be fabricated by sintering the uniform powder compact.

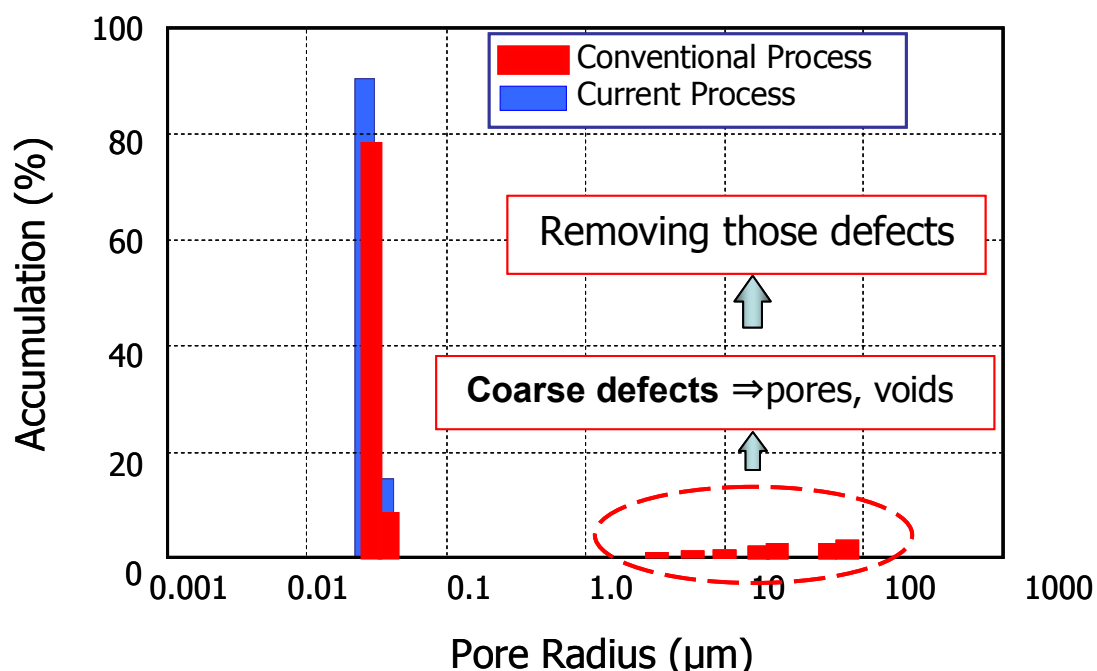


Fig.15 Pore distribution in powder compact prepared with optimized CIP condition in comparison with the conventional powder compact.

9. Optical characterization of high quality laser ceramics

9.1 Irradiation by He-Ne laser

Appearance of high quality laser ceramics is shown in Fig.16. For instance, visible light can be scattered when a ceramic sample includes a certain amount of optical scattering centers such as residual pores and grain boundary phases, which can be observed with our naked eyes from scattering beam.

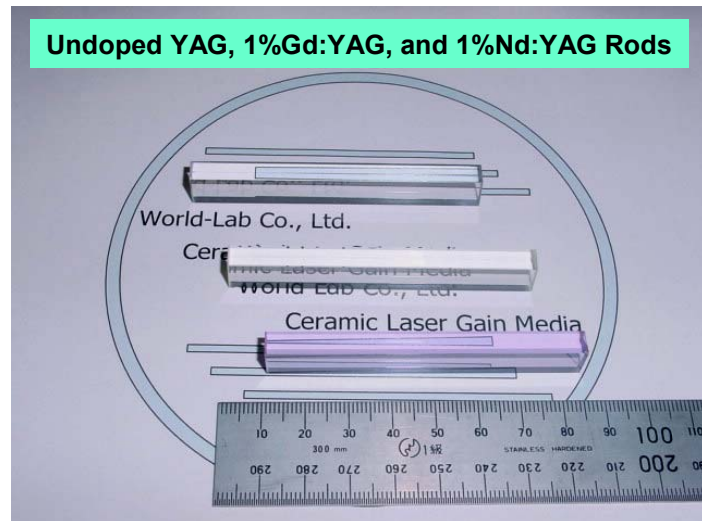


Fig.16 Appearance of high quality laser ceramics.

A commercial He-Ne (633nm) laser was used to readily detect the scattering of the samples in macro level. As seen in Fig.17, scattered beam line was detected by irradiating He-Ne laser across the low quality Nd:YAG sample, but no scattered beam was not observed in high quality Nd:YAG sample.

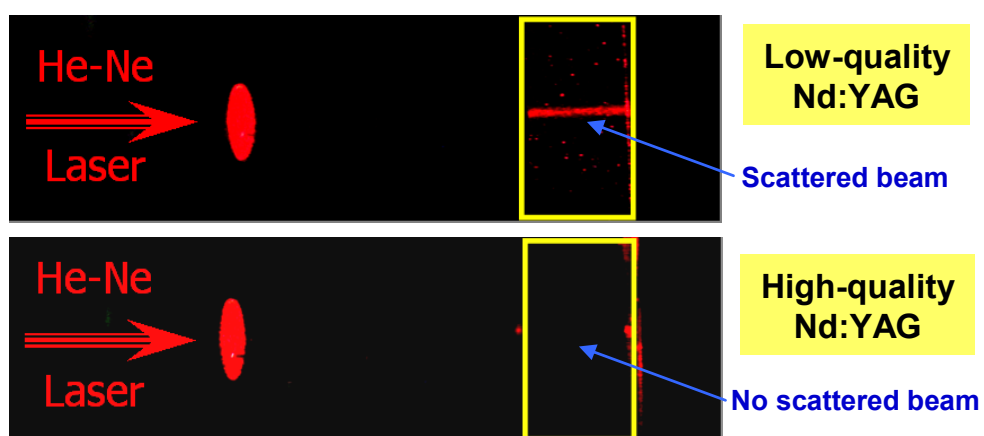


Fig.17 Testing with He-Ne laser irradiation across the specimens.

(Upper) Low quality Nd:YAG sample.

(Lower) High quality Nd:YAG sample achieved by currently improved process.

9.1 Laser scattering tomography

Laser Scattering Tomography (LST) reveals microscopic and submicroscopic particles by elastic scattering of light, in a similar manner than the old method of ultra-microscopy. LST uses an intense laser beam with a wavelength in the transparent region of the investigated material. The beam is focused to the interesting region inside the sample. The irradiated region is imaged by a microscope perpendicularly to the beam, and the arrangement of the scatterers is displayed after electronic data processing (Fig 18). LST gives images with high contrast also from faint objects. The defects are observed inside the bulk without damage of the sample. LST is a well established technique for studies of inclusions (pores or precipitates) and defects decorated by inclusions (such as dislocations). The detectability of defects by this system is dependent upon their scattering powers which are given by defect structure such as refractive index difference, piezo-optical birefringence around dislocations and their shapes. The resolving power of this system is better than that of an objective lens because light scattering is caused by much smaller particles and/or refractive index irregularities than the resolving power of the lens, which is very similar to seeing smoke though we cannot recognize particles in the smoke with our eyes.

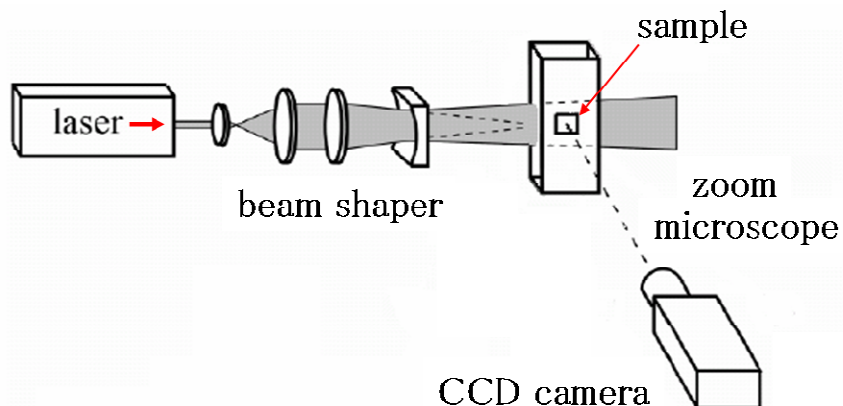


Fig.18 Experimental setup for laser tomography. He-Ne laser or SHG green laser are normally used as an irradiation beam source.

Figure 18 shows the experimental setup. The beam of a He-Ne laser is extended by a beam shaper. The light irradiates the scatterers inside the sample, and it is possible to observe 2D LST images. A microscope images the irradiated scatterers onto a CCD camera. The microscope has a low numerical aperture ($NA=0.08$). This low N.A. restricts the resolution to about $10 \mu m$. An image processing system was used for frame grabbing and digital integration of the video images, and it was then performed by computer.

The following picture (Fig.19) shows a comparison between the LST images obtained in the three YAG samples. Numerous scatterings were detected in low quality Nd:YAG ceramics. But almost no scattering was observed in high quality Nd:YAG ceramics prepared by current process as well as in the commercial Nd:YAG single crystal.

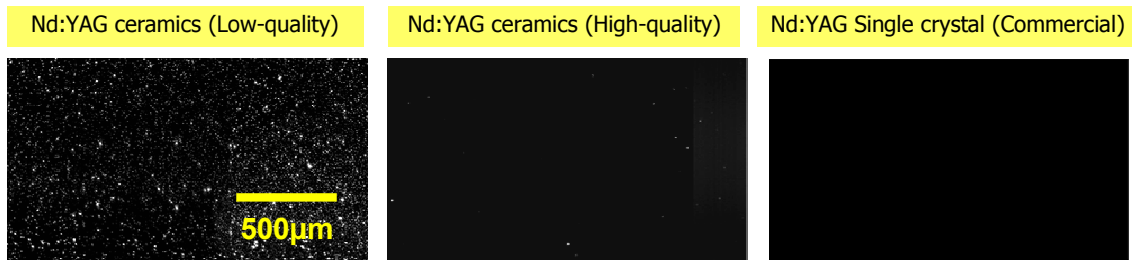


Fig.19 Comparison of density of defects in laser gain media observed by laser scattering tomography.

9.2 Laser induced damage

In order to investigate the relationship between the density of defect and laser induced damage threshold, laser damage test was performed for the above prepared samples. Experimental setup for laser damage test is shown in Fig.20.

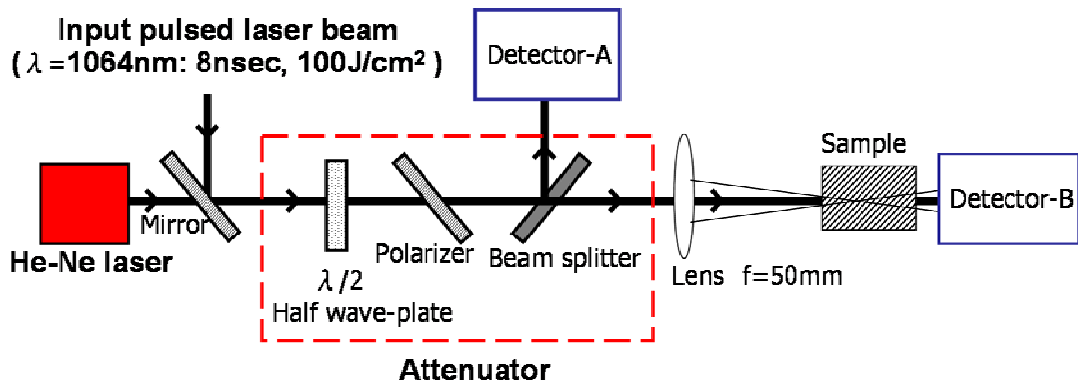


Fig.20 Experimental setup for laser damage test.

The Nd:YAG laser (@1064 nm, 8-9 ns pulse duration, $100\text{J}/\text{cm}^2$) was employed by operating it in the single shot mode. A lens with a focal length of $f=50$ mm was used to focus the laser radiation inside the sample so that the depth of the focal point was located 3 mm under the surface. The energy of the pulses was varied with an attenuator consisting of a polarizer and a half-wave plate. The experiments were performed in accordance with the "1-on-1" procedure, i.e., the damage threshold was measured every time on a new site of the sample. The formation of the bulk damage was identified by the observation of a laser spark.

Light scattering from a coaxial He-Ne laser beam was also employed as a real-time indication of laser-induced damage.

After the laser induced damaging, damaged spot in the YAG materials were observed by a microscope. Microscopic photographs of typical laser damage (cracks) generated in Nd:YAG single crystal and Nd:YAG ceramic are shown in Fig.21 left and right, respectively.

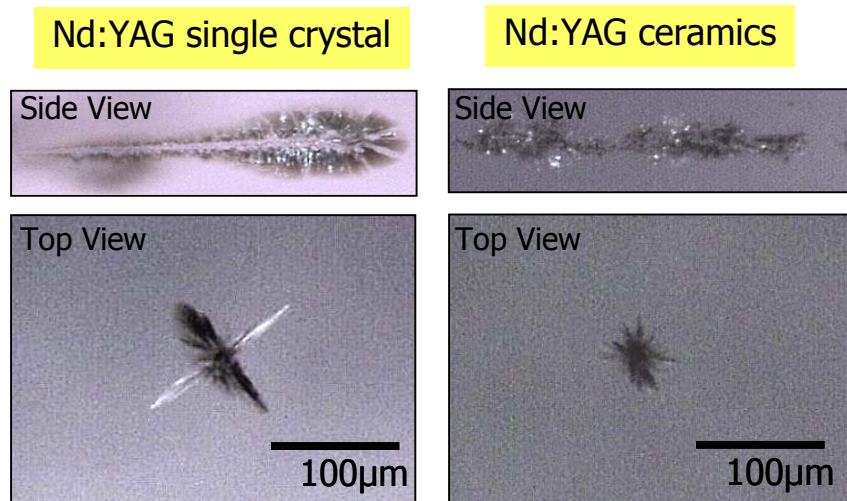


Fig.21 Comparison of laser induced damage generated in each material.

The damage ran parallel to the laser irradiation direction. The crack pattern observed in the single crystal shows two cracks spreading from the central damaged area. These cracks are perpendicular to each other and reflect the four-fold rotation symmetry. On the other hand, regularity was not observed in the crack pattern of YAG ceramics. It was noticed that only small cracks occurred in ceramic materials because grain boundaries in polycrystalline ceramic stopped the extension of cracking. On the other hand, the size of crack in single crystal was found to be larger compared to than in ceramics.

A relationship between the LIDT (laser induced damage threshold) and density of defects (scatterers) were summarized in Fig.22. The LIDT of YAG material increased with the decrease of scattering defect densities. The damage threshold of the high-quality YAG ceramics was almost same as that of single crystal. It was confirmed that the sample with higher density of defect can be easily damaged by high energy laser, and the currently fabricated high quality ceramics are highly resistant to high energy laser.

Thus, the improvement of optical quality by reducing the defect densities can enhance the resistance of YAG ceramics against bulk laser-induced damage, which is leading for the development of high power laser.

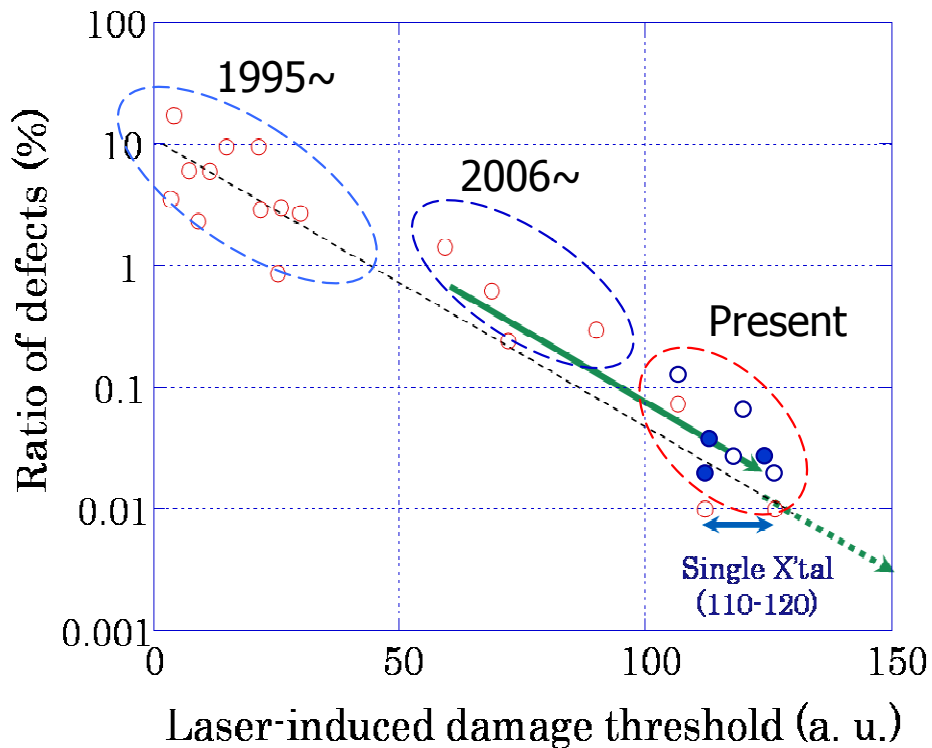


Fig.22 Relationship between LIDT (laser induced damage threshold) and density of defects.

10. Laser oscillation experiment

Four types of 1%Nd:YAG samples; commercial single crystal, the Konoshima ceramics, ceramic lot B1 and ceramic lot B2, having same dimensions and surface polishing quality were prepared for the sake of comparison of laser performance under the same conditions. Here, ceramic lot B1 and B2 were included to confirm the reproducibility of the ceramic process in this project. A schematic diagram of laser oscillation setup is shown in Fig.23. The gain media were pumped at 808 nm by a laser diode.

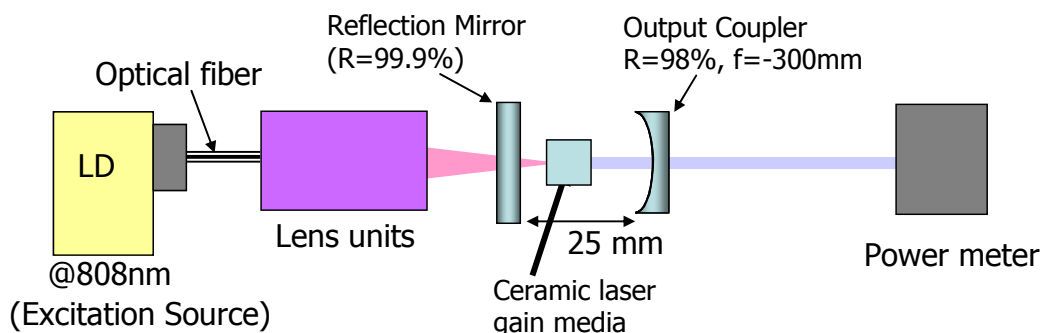


Fig.23 Experimental setup for laser oscillation test.

The laser performances are summarized in Fig 24. Only for the sake of simple comparison in laser performance, the all samples were not AR (anti-reflection) coated. The laser performance of high quality Nd:YAG ceramic samples (lot B1 and B2) currently fabricated in this project was comparable to that of the commercial single crystal and the Konoshima ceramic sample. Although the samples were not AR coated, slope efficiency was as high as approximately 58%, and it is almost equal to theoretical quantum efficiency of Nd:YAG laser.

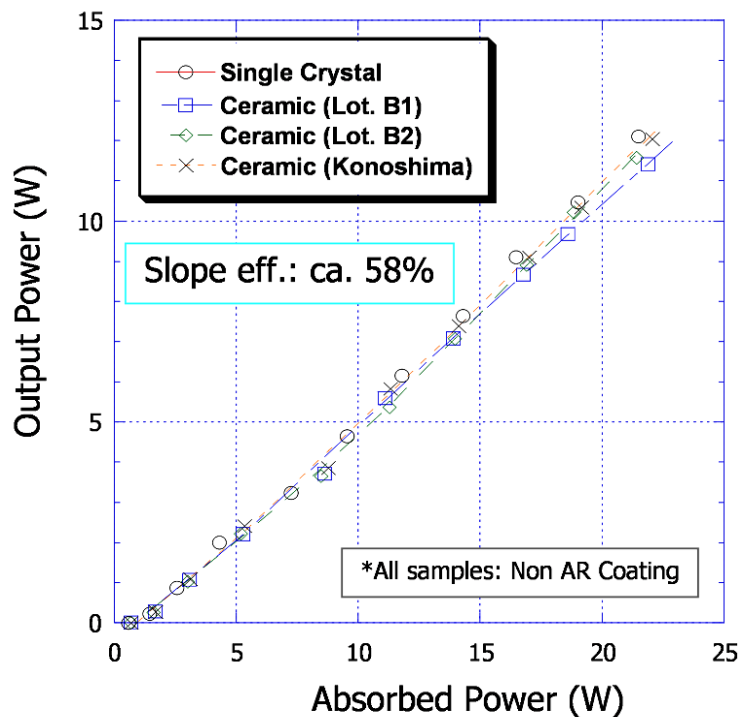


Fig.24 Laser performance of high quality Nd:YAG ceramic samples (lot B1 and B2) currently fabricated in comparison with commercial single crystal and the Konoshima ceramic sample.

Present results showed almost same laser performance as in the previous data, but scattering loss and laser damage resistance were improved significantly. This result suggested that the optical quality of the developed ceramic laser elements is sufficient for the development of high power laser applications.

11. Fabrication of waveguide laser elements

In the second and third year term, waveguide design will be focused because its physical structure is very effective for thermal management in high power laser operation. In addition, by applying ceramic composite technology, the profile (the distribution of active ions) of core waveguide layer can be freely controlled. Therefore, high power output and high beam quality can be expected by creating an advanced waveguide laser.

11.1 Simple waveguide laser element

Preparation steps for the fabrication of simple waveguide structure are shown in Fig.25. Two pieces of undoped YAG were optically polished at one face. And the core waveguide layer with the thickness up to $400\mu\text{m}$ was prepared, and both surfaces were optically polished. Then the polished surfaces were contacted to form a waveguide structure, and it is heated at higher temperature for diffusion bonding. The fabricated simple waveguide elements having 70mm length and 110mm length were shown in Fig.26.

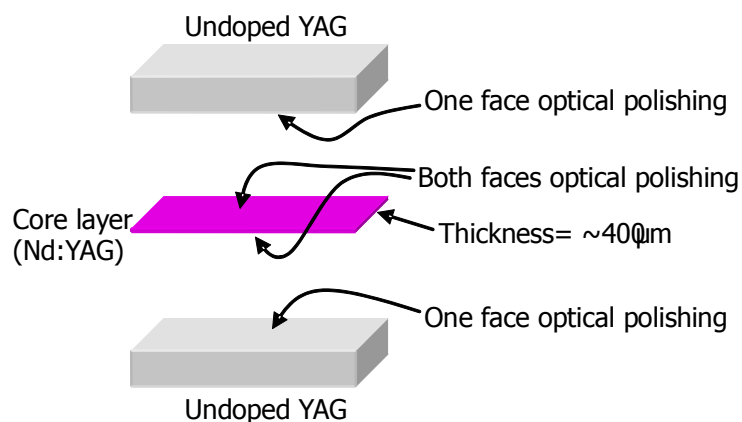


Fig.25 Preparation steps to form a waveguide structure.

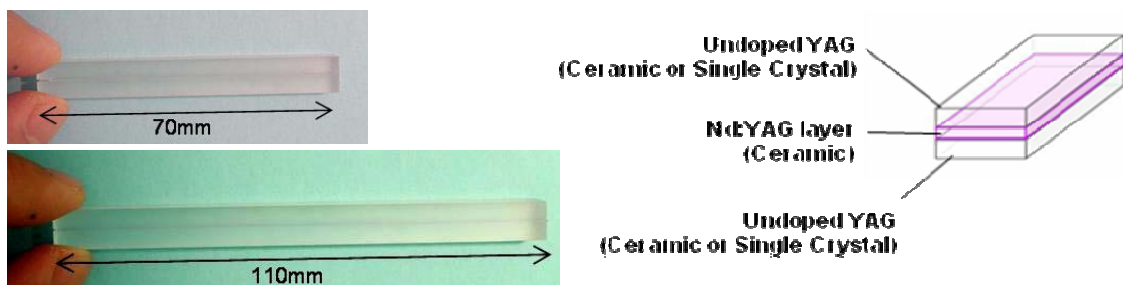


Fig.26 Demonstrated simple waveguide element and its schematic diagram.

11.2 Composite waveguide laser element

In Fig.27 and 28, three-layered (1%Gd:YAG / 1%Nd:YAG / 1%Gd:YAG) and five-layered (1%Gd:YAG / 0.5%Gd,0.5%Nd:YAG / 1%Nd:YAG / 0.5%Gd,0.5%Nd:YAG / 1%Gd:YAG) composite slabs fabricated by advanced ceramic bonding method are shown, respectively. These composites have uniform distribution of refractive index. This idea was proposed by Prof. Byer of Stanford University at the time of kick-off meeting of this project in 2007, November.

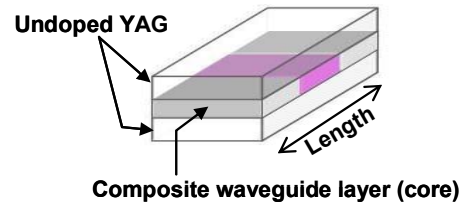
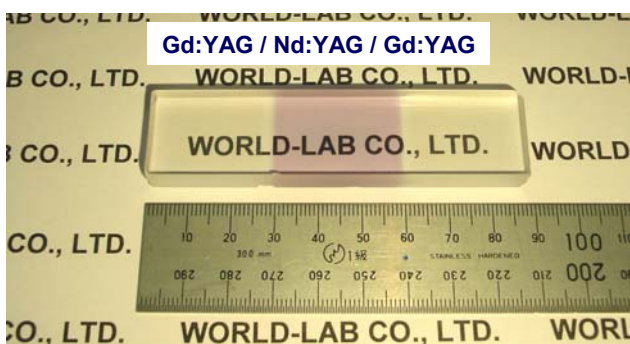


Fig.27 (Left) Recently fabricated three-layered (1%Gd:YAG / 1%Nd:YAG / 1%Gd:YAG) composite, and (right) schematic diagram of advanced waveguide for second year term.

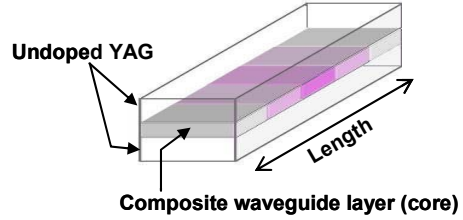
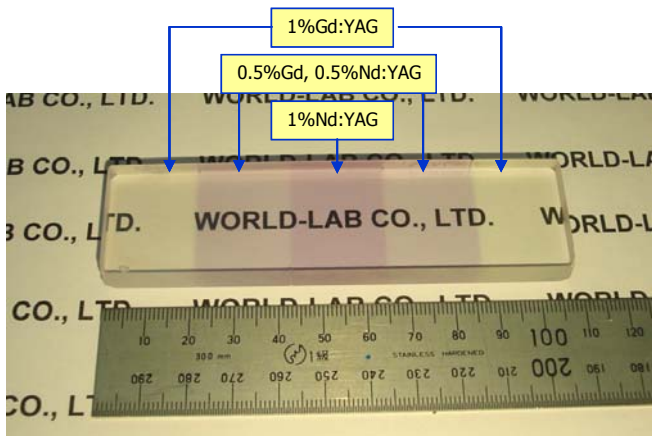


Fig.28 (Left) Recently fabricated five-layered composite and (right) schematic diagram of advanced waveguide element for third year term.

For standard edge-pumped lasers, a gain medium (waveguide core layer) with a uniform doping profile is generally used. However, it is difficult to achieve high output power laser with high beam quality (e.g., TEM₀₀ mode). It is well known that high beam quality can be easily obtained by modifying the ceramic laser gain media with gradient doping profile. By changing the doping level of laser gain ions along the length direction of the slab, the

refractive index also changes along the length direction. When this gain medium with non-uniform refractive index is used in waveguide element, the laser beam quality can be distorted, eliminating the advantage of more pumping and extraction. Therefore, to compensate the refractive index changes due to the changing of laser active (Nd) ions, a certain amount of non-active ions (Gd, Gadolinium) was substituted in Nd:YAG ceramic materials in this project.

These composite will be processed into very thin layer (thickness: up to 400 μm) for the use as a core waveguide layer. Then, by applying the preparation steps shown in Fig.25, advanced waveguide laser elements (see Fig.27 and Fig.28 right side for their schematic diagram) will be fabricated. Finally, the developed laser gain media will be tested for the possibility of high power laser oscillation from 100W to 1kW output level.

12. Conclusions

High optical quality transparent undoped YAG, 1%Gd:YAG, and 1%Nd:YAG ceramic element were successfully fabricated. Uniform microstructures were confirmed and the average grain size was approximately 10 μm . The in-line transmittance of each sample was comparable to that of the commercial single crystal Nd:YAG, and the transmittance at 1064nm was 84%, a theoretical value. Refractive index distribution was confirmed to be very homogeneous by interferometry image, showing straight fringes. Almost no residual pores were recognized under optical microscope and SEM observation. The quality of the optical ceramic gain media was found to improve under macro and microscopic observation. In addition, HR-TEM and EDS analysis results revealed that the fabricated ceramics have almost and ideal and perfect microstructure. Optical characterizations by He-Ne laser showed that the scatter loss is almost zero for the high quality ceramic gain media. In the result, high optical quality ceramics showed high resistance to high energy laser damage. Laser performance with very close to theoretical quantum efficiency was achieved from the developed high quality ceramic gain media, comparable to that of the konoshima ceramics and commercial single crystal. In addition, three-layered and five-layered composites for the core layer of advanced waveguide elements were successfully fabricated by direct forming method.

13. Future plan

Fabrication of waveguide laser elements with simple waveguide layer and with composite waveguide layers (three-layered and five-layered core, refer Fig.26, 27 and 28) will be tested by new ceramic bonding technology. Then, the developed laser gain media will be tested for the possibility of high power laser oscillation test from 100W to 1kW output level.

LIST OF MANUSCRIPTS SUBMITTED OR PUBLISHED UNDER AFOSR/AOARD SPONSORSHIP DURING THIS REPORTING PERIOD:

A part of the project was slightly introduced in this publication (review article).

1. Akio Ikesue and Yan Lin Aung, "Ceramic laser materials", Nature Photonics, VOL.2, December (2009) www.nature.com/naturephotonics

Acknowledgement

This work was supported by AFOSR/AOARD through funds received from Roppongi office, Tokyo AOARD Grant Number: 08- 4043.